10-9-2017

How accurate are satellite estimates of precipitation over the north Indian Ocean?

Satya Prakash
CUNY New York City College of Technology

M. R. Ramesh Kumar
National Institute of Oceanography

Simi Mathew
National Institute of Ocean Technology

R. Venkatesan
National Institute of Ocean Technology

Recommended Citation
Satya Prakash, M. R. Ramesh Kumar, S. Mathew, and R. Venkatesan 2017: How accurate are satellite estimates of precipitation over the north Indian Ocean?, Theoretical and Applied Climatology, doi:10.1007/s00704-017-2287-2.

How accurate are satellite estimates of precipitation over the north Indian Ocean?

Satya Prakash[1,#], M. R. Ramesh Kumar[2], Simi Mathew[3], and R. Venkatesan[3]

[1]New York City College of Technology, City University of New York, NY, USA

[2]National Institute of Oceanography, Dona Paula, Goa, India

[3]National Institute of Ocean Technology, Chennai, India

[#]*Current Affiliation:* Divecha Centre for Climate Change,

Indian Institute of Science, Bengaluru, India

Corresponding Author's Address:

Dr. M. R. Ramesh Kumar

Physical Oceanography Division,

National Institute of Oceanography,

Dona Paula, Goa – 403 004, India.

Email: kramesh@nio.org

Accepted in *Theoretical and Applied Climatology (October 2, 2017)*

doi:10.1007/s00704-017-2287-2

ABSTRACT

Following the launch of the Global Precipitation Measurement (GPM) Core Observatory in early 2014, motivated from the successful Tropical Rainfall Measurement Mission (TRMM) satellite, an advanced and sophisticated global multi-satellite precipitation product – Integrated Multi-satellitE Retrievals for GPM (IMERG) was released at finer spatio-temporal scales. This precipitation product has been upgraded recently after several refinements and supposed to be superior to other existing global or quasi-global multi-satellite precipitation estimates. In the present study, IMERG precipitation is comprehensively evaluated for the first time against moored buoy observations over the north Indian Ocean at hourly scale for the study period of March 2014 to December 2015. IMERG precipitation performs considerably better over the Bay of Bengal than the Arabian Sea in both detection and estimation. The systematic error in IMERG is appreciably lower by about 14%, however, it generally overestimates in-situ precipitation and also exhibits noticeable false alarms. Furthermore, IMERG essentially shows an improvement over the TRMM Multi-satellite Precipitation Analysis (TMPA) at a daily scale over the north Indian Ocean. IMERG precipitation estimates show overall promising error characteristics, but there is still a need of substantial efforts for improvement in the satellite-based precipitation estimation algorithms especially over data sparse regions such as north Indian Ocean.

1. Introduction

Precipitation is one of the most crucial parameters in the global hydrological cycle, which plays vital role in the Earth's energy and water balance. About 78% of the global precipitation occurs over the vast oceans (Trenberth et al. 2007), thus reliable estimates of oceanic precipitation are critical for better understanding of the global water cycle and subsequently for

the global climate system. Precipitation also plays a key role in freshwater flux and sea surface salinity variations (Ramesh Kumar and Schulz 2002; Prakash et al. 2012). However, in-situ observations of precipitation over the global oceans are essentially heterogeneous and sparse, limiting its applicability for global and regional scale applications (Ramesh Kumar and Prasad 1997; Ramesh Kumar et al. 2006; Prakash et al. 2013; Prakash and Gairola 2014). The Ocean Rain And Ice-phase precipitation measurement Network (OceanRAIN; Klepp 2015) project is aimed to better understand the global oceanic precipitation characteristics and for the validation of satellite, reanalysis and numerical model precipitation datasets. OceanRAIN provides comprehensive estimates of oceanic rain, snow and mixed-phase precipitation using optical disdrometers onboard research vessels since 2010. However, the Indian Ocean is not yet covered by the OceanRAIN. Alternatively, remote sensing satellite-based retrievals of precipitation are now capable to provide the global comprehensive estimates at regular spatio-temporal intervals in near real-time with considerable accuracy (Grassl et al. 2000; Kidd and Levizzani 2011; Kucera et al. 2013; Behrangi et al. 2014; Tapiador et al. 2017).

The Global Precipitation Measurement (GPM) Core Observatory, built upon the heritage of the Tropical Rainfall Measuring Mission (TRMM) satellite, was launched on 27 February 2014 to provide unified high-resolution global rain as well as snow observations at better accuracy in near-real time (Hou et al. 2014; Liu et al. 2017). The GPM-based multi-satellite precipitation estimates namely, Integrated Multi-satellitE Retrievals for GPM (IMERG; Huffman et al. 2017), were released in early 2015 that benefits from the relative advantages of precipitation estimates from contemporary microwave and infrared sensors. This high-resolution advanced precipitation product is now available half-hourly at 0.1° latitude/longitude in three distinct modes – early, late, and final runs based on latency and accuracy. This product is

considered as the next-generation of multi-sensor precipitation data that takes advantages of three existing multi-satellite precipitation estimation algorithms and is superior to other TRMM-era multi-satellite precipitation estimates (Liu 2016; Prakash et al. 2016; Wang et al. 2017). IMERG final run product is derived primarily for the research purposes and available since 12 March 2014 with a latency of about 3 months. This precipitation product uses available gauge analysis over the land for bias correction along with multi-satellite precipitation estimates.

The existing IMERG version 3 precipitation products underwent retrospective processing and version 4 products were released in March 2017. Version 4 uses a homogeneous algorithm to compute precipitation estimates from all passive microwave sensors and benefits from additional remote sensing data over the globe (Huffman et al. 2017). In this study, precipitation estimates from IMERG final run version 4 product is first time extensively assessed over the north Indian Ocean using buoy measurements at hourly scale for the period of March 2014 to December 2015. It is to be noted that the precipitation over this oceanic region has paramount impact on the surrounding landmasses at distinct scales (Ramesh Kumar and Sreejith 2005; Ramesh Kumar et al. 2005, 2006, 2009; Pai et al. 2016). For instance, the sea surface temperature, moisture and wind over the Arabian Sea is crucial for the onset and progress of the southwest monsoon over India. The low-level monsoon jet carries moisture from the Arabian Sea and interacts with the complex orography of the Western Ghats, resulting into heavy rainfall along these regions during the monsoon period (June – September). Similarly, most of the monsoon lows and depressions form in the Bay of Bengal, which generally move northwestward and cause substantial monsoon rainfall over the central India. Additionally, the intraseasonal variations of the monsoon rainfall is closely associated with the rainfall over the north Indian Ocean. The performance of this

GPM-based precipitation product is also evaluated in comparison to a TRMM-era multi-satellite estimate at daily scale for the southwest monsoon period of 2014 and 2015.

2. Data and Methods

2.1 Multi-satellite precipitation estimates

The basic objective of the IMERG algorithm is to inter-calibrate and merge all available TRMM- and GPM-era satellite microwave and infrared precipitation estimates at finer spatio-temporal scales over the globe (Huffman et al. 2017). The GPM Core satellite acts as a calibrator for all the input satellite-based precipitation products. This multi-satellite precipitation estimation algorithm utilizes the relative merits of the TRMM Multisatellite Precipitation Analysis (TMPA; Huffman et al. 2010), the Climate Prediction Center Morphing – Kalman Filter (CMORPH-KF; Joyce et al. 2011) and the Precipitation Estimation from Remotely Sensed Information using Artificial Neural Networks – Cloud Classification System (PERSIANN-CCS; Hong et al. 2004) schemes. This system runs twice in near-real time (early and late runs) and once after the availability of monthly rain gauge analysis over the global land areas (final run). Half-hourly IMERG final run version 4A precipitation estimates for March 2014 to December 2015 were used. Furthermore, daily TMPA-3B42 research version 7 precipitation estimates for the southwest monsoon season (June – September) of 2014 and 2015 were also used to assess the relative performance of both TRMM- and GPM-era multi-satellite products. Since the TMPA product is proven to be the best TRMM-era multi-satellite precipitation product (Prakash et al. 2014, 2015b, 2015c; Maggioni et al. 2016), we did not consider other TRMM-based products in this study.

2.2 Moored buoy precipitation data

In order to better understand the observed variability of the ocean dynamics at different spatio-temporal scales and their association with the monsoons and tropical cyclones, the National Institute of Ocean Technology (NIOT) at Chennai, India deployed seven moored buoys in the Bay of Bengal and five buoys in the Arabian Sea under its Ocean Observation Program (Venkatesan et al. 2013; Ramesh Kumar et al. 2017). These buoys are known as the Ocean Moored buoy Network for Northern Indian Ocean (OMNI) and are operational since May 2011 and October 2012 in the Bay of Bengal and Arabian Sea, respectively. These moored buoys provide the measurement of precipitation, wind, humidity, air temperature, radiation and vertical profiles of salinity, temperature and current. OMNI buoys are equipped with RM Young capacitance type gauge mounted at 3-meter height above the sea surface. These buoys measure precipitation ranging 0-50 mm with an accuracy of ±1 mm, sampling rate of 1 Hz, and sampling period of 1-minute (Venkatesan et al. 2013). The precipitation data are recorded at 2-minute interval. A suitable quality control was done with the raw precipitation data, such as removal of negative rain rate due to noise during non-precipitating conditions, elimination of siphon events, etc. for the computation of hourly precipitation rate. Serra et al. (2001) studied the rain gauge error estimates using the Autonomous Temperature Line Acquisition System (ATLAS) buoys in the tropical Pacific and Atlantic Oceans and reported the estimated error of 1.3 mm h^{-1} for 1-min real-time rain data, 0.4 mm h^{-1} for 10-min data, and 0.03 mm h^{-1} for daily rain rates without taking wind effects into account. Precipitation observations from these twelve buoys in the north Indian Ocean (Fig. 1) were used to assess the accuracy of IMERG precipitation product at hourly timescale. Additionally, daily precipitation observations from two Research Moored Array for African–Asian–Australian Monsoon Analysis and Prediction (RAMA; McPhaden et al. 2009)

buoys located in the Bay of Bengal (11°N-90°E and 14°N-90°E) for the southwest monsoon season of 2014 and 2015 were also used in this study. However, these OMNI and RAMA buoys do not provide any information about the precipitation type and phase (e.g., convective/stratiform rainfall, liquid/solid/mixed phase).

2.3 Methodology

In this study, an evaluation is performed at each buoy station separately because the density of OMNI buoys is rather sparse. It needs to be mentioned here that precipitation measurement principles are completely different for both in-situ and satellite estimates. Satellite provides precipitation measurement for an area at a specific time, whereas buoys provide point measurement. The precipitation corresponding to the nearest satellite grid of buoy observations were considered for collocation followed by proper quality checks. There exists a considerable error in buoy precipitation due to wind-induced undercatch of gauges, and due to evaporation during the daytime (Koschmieder 1934; Serra et al. 2001 Sapiano and Arkin 2009). However, there is no additional correction applied to the buoy precipitation data in this study. Hourly precipitation was computed from half-hourly IMERG product. The collocated database for each buoy location were prepared by taking proportionate precipitating and non-precipitating events into account. Since the Bay of Bengal and the Arabian Sea exhibits distinct meteorological and oceanic features although situated in the same latitudinal belt (Ramesh Kumar and Sreejith 2005), the assessment was done for both the regions of the north Indian Ocean separately. The Bay of Bengal receives large precipitation, and freshwater from the river discharge. However, the Arabian Sea gets more evaporation than precipitation. Hence, the sea surface salinity of the Bay

of Bengal is less than the Arabian Sea, and mixed layer depth is deeper in the Arabian Sea as compared to the Bay of Bengal.

For the evaluation of multi-satellite estimates against moored buoy observations, conventional continuous error metrics such as correlation coefficient (r), bias, root-mean-square error (RMSE), empirical cumulative distribution function (CDF) were computed (Prakash and Gairola 2014). The mean-square error (MSE) in the multi-satellite precipitation estimates were further decomposed into systematic and random error components using additive error model (AghaKouchak et al. 2012; Prakash et al. 2015a) given by equation (1). The systematic error is generally due to algorithm characteristics and could be minimized using suitable statistical methods.

$$MSE = MSE_{sys} + MSE_{rand} = \frac{\sum_{i=1}^{N} \left(P_{sat}^{¿} - P_{obs} \right)^2}{N} + \frac{\sum_{i=1}^{N} \left(P_{sat} - P_{sat}^{¿} \right)^2}{N} \qquad (1)$$

$$\text{with} \quad P_{sat}^{¿} = a \times P_{obs} + b \qquad (2)$$

where, N be the number of collocations, P_{sat} and P_{obs} be the precipitation estimates from multi-satellite and moored buoys, respectively. a and b are slope and intercept, respectively. Additionally, the representativeness error resulting from the different spatial resolutions and measuring principles of gauges and satellites could strongly contribute to the differences between both datasets.

Furthermore, four categorical indices probability of detection (POD), false alarm ratio (FAR), missing rate (MR), and critical success index (CSI) were used to assess the potential of multi-satellite estimates for precipitation detection as compared to moored buoy observations.

$$POD = \frac{H}{H + M} \qquad (3)$$

$$FAR = \frac{F}{H + F} \qquad (4)$$

$$MR = \frac{M}{H + M} \qquad (5)$$

$$CSI = \frac{H}{H + F + M} \qquad (6)$$

In equations (3) – (6), *H* represents the number of events when both satellite and buoy detected precipitation, *F* be the number of events when satellite detected precipitation but buoy didn't, and *M* be the number of events when buoy detected precipitation but satellite could not. All these four indices range from 0 to 1 with an ideal score as 1 for POD and CSI, and 0 for FAR and MR.

3. Results and Discussions

Fig. 2 shows the mean seasonal precipitation from IMERG product for the pre-monsoon (March – May), monsoon (June – September) and post-monsoon (October – December) seasons

over the north Indian Ocean and adjoining land regions. These spatial maps of precipitation at 0.1° latitude/longitude are derived from two-years (2014 and 2015) of IMERG research product. The well-known features of precipitation over the north Indian Ocean (e.g., high precipitation off the southwest coast of India and near Myanmar coast, during monsoon season) are captured adequately from this multi-satellite product. In general, the Arabian Sea receives less precipitation than the Bay of Bengal that leads to more saline water in the Arabian Sea. During the pre-monsoon season, precipitation is primarily restricted near the equatorial Indian Ocean which moves northward during the monsoon season associated with the movement of the inter-tropical convergence zone. The Bay of Bengal usually remains active during the monsoon season due to formation of lows/depressions. The precipitation systems start to move again southward during the post-monsoon season and the southern part of the Bay of Bengal gets considerable precipitation. The intermittent development of the tropical cyclones during this season in the north Indian Ocean also lead to substantial precipitation.

Fig. 3 presents the time-series comparison of hourly precipitation from IMERG and OMNI buoy observations, and three-hourly precipitation from TMPA for three different cases over the Bay of Bengal and Arabian Sea. First, we choose 8-11 October 2014 because an extremely severe cyclonic storm ‘Hudhud’ formed over the Bay of Bengal during this time and made landfall in India. This storm brought extensive damage along the east coast of India. Second, we select 2-7 November 2014 because a deep depression formed over the Bay of Bengal during this period. Third, we choose 5-10 June 2015 because a cyclonic storm ‘Ashobaa’ developed over the Arabian Sea during this period, which caused delayed onset of the Indian summer monsoon. Although the heavy precipitation associated with these three cases are generally detected well by the IMERG product, the magnitude and pattern have notable

differences. IMERG has higher magnitudes of heavy precipitation as compared to buoy observations over the Bay of Bengal. It might be related to the wind-induced undercatch of gauges during heavy precipitation events. Despite TMPA shows similar precipitation variation as IMERG, the magnitude of heavy precipitation by TMPA is less than IMERG. It is primarily due to coarser spatial and temporal resolutions of TMPA as compared to IMERG estimates. In general, TMPA has lower magnitudes of heavy precipitation as compared to buoy observations.

In this section, hourly IMERG precipitation estimates are evaluated against each OMNI buoy locations for the period of March 2014 to December 2015. The different error metrics for the Arabian Sea and Bay of Bengal are presented separately in Table 1. The number of collocated observations are higher over the Bay of Bengal than the Arabian Sea due to two reasons. Firstly, Bay of Bengal has seven OMNI buoys as compared to five buoys in the Arabian Sea. Secondly, the Arabian Sea does not receive precipitation throughout the year whereas the Bay of Bengal receives precipitation most of the time except during the winter (January-February) season. The continuous error metrics (e.g., correlation and bias) show similarity in both the basins. However, IMERG shows larger RMSE in the Arabian Sea than in the Bay of Bengal. The error decomposition shows that the systematic error in IMERG is noticeably smaller in both the basins and the contribution of random component is substantial in the GPM-based multi-satellite estimate.

Fig. 4 shows the capability of IMERG product in the detection of rainy and non-rainy events. The categorical metrics show better performance by IMERG in the precipitation detection over the Bay of Bengal than the Arabian Sea. Though IMERG is capable to detect precipitation events due to high POD in both the basins of the north Indian Ocean, it has considerably high FAR and MR. The satellite-based precipitation estimates represent a grid

(~100 km^2 area in case of IMERG) rather than a single point, which might be one of the reasons behind this discrepancy. Moreover, light precipitation below the sensitivity threshold of 0.2 mm hr^{-1} from IMERG could explain some of the MR.

The capability of IMERG in capturing different ranges of precipitation over the north Indian Ocean is also assessed through frequency distribution (Fig. 4). IMERG notably overestimates precipitation across the range in both the basins. However, the overestimation of frequent light precipitation (0.2-1 mmh^{-1}) by the satellite-based estimate is more pronounced compared to other precipitation ranges. The satellite-based precipitation is representative of a large area (~10 km × 10 km for IMERG), and if small-scale showers move within the IMERG box but that do not move over the exact buoy's location could substantially contribute to the apparent overestimation of light precipitation by IMERG against the buoys. In addition, extreme precipitation (≥20 mmh^{-1}) is also overestimated by the IMERG estimate. IMERG is in very good agreement with buoy observations for the precipitation range of 5-20 mmh^{-1}. Fig. 5 presents the empirical CDF of precipitation events captured from IMERG and OMNI buoy observations in the Arabian Sea and Bay of Bengal, which also supports the systematic overestimation by IMERG. It is assumed that the stratiform precipitation is represented well as compared to the convective precipitation by the gauge. However, there is no information about the precipitation type over the north Indian Ocean unlike OceanRAIN project primarily over the Atlantic Ocean.

The orbits of TRMM and GPM satellites were chosen in such a way that they could enable to study the diurnal variability of precipitation. As diurnal variation of precipitation is primarily associated with the underlying atmospheric dynamics and geographical features, reliable knowledge of the diurnal cycle is vital for a wide range of applications. Ramesh Kumar et al. (2006) investigated the diurnal cycle of precipitation in the equatorial Indian Ocean using

hourly TRITON buoy observations in 2002 and found that the precipitation peaked in the late evening during winter, summer and fall seasons and during early morning hours of spring season. Here, the diurnal cycle from hourly IMERG and buoy observations are investigated at two locations in the north Indian Ocean for the month of August 2014. One buoy located in the Arabian Sea and one buoy located in the Bay of Bengal are selected for this analysis. Fig. 6 presents the mean hourly precipitation rate from IMERG and buoy observations averaged for a month and their respective standard deviations for both buoy locations. Three-hourly TMPA product is also considered at available hours. There are considerable differences between satellite and moored buoy observations in capturing the diurnal cycle. In general, buoy observations show larger standard deviation than satellite estimates during the peak precipitation hours. TMPA has comparatively smaller standard deviation than IMERG and buoy observations. The agreement between satellite and in-situ observations becomes notably better with increasing temporal averaging (e.g., hourly to daily).

Furthermore, daily precipitation estimates from IMERG and TMPA are evaluated with RAMA buoy observations over the Bay of Bengal for the monsoon period of 2014 and 2015. This analysis is performed with an objective of relative comparison of the GPM- and TRMM-based multi-satellite precipitation estimates. Although, the TMPA algorithm is benchmark for the IMERG algorithm, there are some differences between both multi-satellite precipitation estimates. These differences are primarily due to calibration, input sensors and retrieval methods (Liu 2016; Huffman et al. 2017). IMERG algorithm benefits from the three multi-satellite algorithms including TMPA, CMORPH-KF, and PERSIANN-CCS algorithms. Fig. 7 shows the scatter plots between satellite and moored buoy daily precipitation observations. IMERG shows a better correlation, and reduced bias and RMSE than TMPA. The overestimation of precipitation

by TMPA research product as compared to RAMA buoy observations over the north Indian Ocean was also reported by Prakash and Gairola (2014). However, the overestimation of precipitation is marginally improved by IMERG over TMPA. As expected, IMERG product also shows an improvement in precipitation detection as compared to TMPA product. These results convincingly suggest a considerable improvement in precipitation detection and estimation by IMERG as compared to TMPA over the north Indian Ocean, consistent with other parts of the globe (Liu, 2016; Prakash et al., 2016; Wang et al., 2017). The improvement in IMERG over TMPA is basically due to advanced instrumentation in GPM Core Observatory as compared to TRMM satellite as well as better precipitation retrieval algorithm (Hou et al. 2014; Huffman et al. 2017). The increased spatial resolution of IMERG with respect to TMPA might also reduce the representativeness error resulting from the differences due to point-to-area comparison.

4. Conclusion

Accurate estimates of precipitation over the tropical Indian Ocean are crucial for better understanding of the South Asian monsoon variability and the global water cycle. The recent updated version of GPM-based high-resolution multi-satellite product, IMERG research product V04A, was critically evaluated using OMNI moored buoy observations over the Arabian Sea and Bay of Bengal. The assessment was done at hourly scale for the period between March 2014 and December 2015. IMERG was capable to capture most of the large-scale features of oceanic precipitation adequately. Even though this multi-satellite product was able to detect precipitation notably, it showed substantial false alarms and missing rate. Additionally, IMERG overestimated precipitation across the range over both Arabian Sea and Bay of Bengal, but the overestimation was more pronounced for light and extreme precipitation events. Also, diurnal variations of

precipitation were not captured adequately by the IMERG product. Furthermore, IMERG research product was inter-compared with TMPA research product at daily scale for the southwest monsoon period of 2014 and 2015, which showed a noticeable improvement in IMERG over TMPA in precipitation detection and estimation over the north Indian Ocean. However, there exists a considerable representativeness error due to point-to-area comparison and differences in precipitation measuring principles from the buoys and satellites. The buoy observations has also some limitations primarily due to wind and sea surface effects. The observations of precipitation type and phase are also crucial over the Indian Ocean for the comprehensive understanding of the error estimates in the satellite-based precipitation products. In addition, there is essentially a need of augmentation of moored buoys over the Indian Ocean to better understand its underlying atmospheric and oceanic dynamics.

Acknowledgements: The IMERG and TMPA precipitation data sets obtained from the FTP server hosted by the Precipitation Processing System, and the RAMA buoy data obtained from the Tropical Atmosphere Ocean Project Office of NOAA Pacific Marine Environmental Laboratory are thankfully acknowledged. M. R. Ramesh Kumar, Simi Mathew, and R. Venkatesan would like to thank the Directors of CSIR-NIO, Goa, and ESSO-NIOT, Chennai, for their support and encouragement, and to the Ministry of Earth Sciences for the funding support for the Ocean Observation Network Programme. They also thank the anonymous reviewers for constructive comments, and to the staff who supported the field measurements. CSIR-NIO contribution number is 6112.

References

AghaKouchak A, Mehran A, Norouzi H, Behrangi A (2012) Systematic and random error components in satellite precipitation data sets. Geophys Res Lett 39:L09406. doi:10.1029/2012GL051592.

Behrangi A, Stephens G, Adler RF, Huffman GJ, Lambrigtsen B, Lebsock M (2014) An update on the oceanic precipitation rate and its zonal distribution in light of advanced observations from space J Clim 27:3957-3965. doi:10.1175/JCLI-D-13-00679.1.

Grassl H, Jost V, Ramesh Kumar MR, Schulz J, Bauer P, Schlussel P (2000) The Hamburg Ocean-Atmosphere Parameters and Fluxes from Satellite Data (HOAPS): A climatological atlas of satellite-derived air-sea interaction parameters over the Oceans. Report No. 312, Max-Planck-Instut fur Meteorologie, Hamburg, Germany, 132 pp.

Hong Y, Hsu KL, Sorooshian S, Gao X (2004) Precipitation estimation from remotely sensed imagery using an artificial neural network cloud classification system. J Appl Meteorol 43:1834-1852. doi:10.1175/JAM2173.1.

Hou AY, Kakar RK, Neeck S, Azarbarzin AA, Kummerow CD, Kojima M, Oki R, Nakamura K, Iguchi T (2014) The Global Precipitation Measurement mission. Bull Amer Meteorol Soc 95:701-722. doi:10.1175/BAMS-D-13-00164.1.

Huffman GJ, Bolvin DT, Braithwaite D, Hsu K, Joyce R, Kidd C, Nelkin EJ, Sorooshian S, Tan J, Xie P (2017) NASA Global Precipitation Measurement (GPM) Integrated Multi-satellitE Retrievals for GPM (IMERG). Algorithm Theoretical Basis Document (ATBD) version 4.6, NASA/GSFC, Greenbelt, MD, USA, 32 pp.

Huffman GJ, Adler RF, Bolvin DT, Nelkin EJ (2010) The TRMM multi-satellite precipitation analysis (TMPA). [edited by F. Hossain and M. Gebremichael] In Satellite applications for surface hydrology, Springer, p. 3-22. doi:10.1007/ 978- 90- 481- 2915- 7_1.

Joyce, R., Xie P, Janowiak JE (2011) Kalman filter-based CMORPH. J Hydrometeorol 12:1547-1563. doi:10.1175/JHM-D-11-022.1.

Kidd C, Levizzani V (2011) Status of satellite precipitation retrievals. Hydrol Earth Syst Sci 15:1109-1116. doi:10.5194/hess-15-1109-2011.

Klepp C (2015) The oceanic shipboard precipitation measurement network for surface validation – OceanRAIN. Atmos Res 163:74-90. doi:10.1016/j.atmosres.2014.12.014.

Koschmieder H (1934) Methods and results of definite rain measurements. Mon Wea Rev 62:5-7.

Kucera PA, Ebert EE, Turk FJ, Levizzani V, Kirschbaum D, Tapiador FJ, Loew A, Borsche M (2013) Precipitation from space: Advancing Earth system science. Bull Amer Meteorol Soc 94:365-375. doi:10.1175/BAMS-D-11-00171.1.

Liu Z, Ostrenga D, Vollmer B, Deshong B, Macritchie K, Greene M, Kempler S (2017) Global Precipitation Measurement mission products and services at the NASA GES DISC. Bull Amer Meteorol Soc 98:437-444. doi:10.1175/BAMS-D-16-0023.1.

Liu Z (2016) Comparison of Integrated Multisatellite Retrievals for GPM (IMERG) and TRMM Multisatellite Precipitation Analysis (TMPA) monthly precipitation products: Initial results. J Hydrometeorol 17:777-790. doi:10.1175/JHM-D-15-0068-1.

Maggioni V, Meyers PC, Robinson MD (2016) A review of merged high-resolution satellite precipitation product accuracy during the Tropical Rainfall Measuring Mission (TRMM) era. J Hydrometeorol 17:1101-1117. doi:10.1175/JHM-D-15-0190-1.

McPhaden MJ, Meyers G, Ando K, Masumoto Y, Murty VSN, Ravichandran M, Syamsudin F, Vialard J, Yu L, Yu W (2009) RAMA: The Research Moored Array for African–Asian–Australian Monsoon Analysis and Prediction. Bull Amer Meteorol Soc 90:459-480. doi:10.1175/2008BAMS2608.1.

Pai DS, Sridhar L, Ramesh Kumar MR (2016) Active and break events of Indian summer monsoon during 1901-2014. Clim Dyn 46:3921-3939. doi:10.1007/s00382-015-2813-9.

Prakash S, Mahesh C, Gairola RM (2012) Observed relationship between surface freshwater flux and salinity in the North Indian Ocean. Atmos Oceanic Sci Lett 5:163-169. doi:10.1080/16742834.2012.11446984.

Prakash S, Mahesh C, Gairola RM (2013) Comparison of TRMM Multisatellite Precipitation Analysis (TMPA)-3B43 version 6 and 7 products with rain gauge data from ocean buoys. Remote Sens Lett 4:677-685. doi:10.1080/2150704X.2013.783248.

Prakash S, Sathiyamoorthy V, Mahesh C, Gairola RM (2014) An evaluation of high-resolution multisatellite rainfall products over the Indian monsoon region. Int J Remote Sens 35:3018-3035. doi:10.1080/01431161.2014.894661.

Prakash S, Gairola RM (2014) Validation of TRMM-3B42 precipitation product over the tropical Indian Ocean using rain gauge data from the RAMA buoy array. Theor Appl Climatol 115:451-460. doi:10.1007/s00704-013-0903-3.

Prakash S, Mitra AK, AghaKouchak A, Pai DS (2015a) Error characterization of TRMM Multisatellite Precipitation Analysis (TMPA-3B42) products over India for different seasons. J Hydrol 529:1302-1312. doi:10.1016/j.jhydrol.2015.08.062.

Prakash S, Mitra AK, Momin IM, Gairola RM, Pai DS, Rajagopal EN, Basu S (2015b) A review of recent evaluations of TRMM Multisatellite Precipitation Analysis (TMPA) research products against ground-based observations over Indian land and oceanic regions. Mausam 66:355-366.

Prakash S, Mitra AK, Momin IM, Pai DS, Rajagopal EN, Basu S (2015c) Comparison of TMPA-3B42 versions 6 and 7 precipitation products with gauge-based data over India for the southwest monsoon period. J Hydrometeorol 16:346-362. doi:10.1175/JHM-D-14-0024.1.

Prakash S, Mitra AK, AghaKouchak A, Liu Z, Norouzi H, Pai DS (2016) A preliminary assessment of GPM-based multi-satellite precipitation estimates over a monsoon dominated region. J Hydrol doi:10.1016/j.jhydrol.2016.01.029.

Ramesh Kumar MR, and Prasad TG (1997) Annual and interannual variation of precipitation over the tropical Indian Ocean. J Geophys Res 102(C8):18519-18527. doi:10.1029/97JC00979.

Ramesh Kumar MR, Schulz J (2002) Analysis of freshwater flux climatology over the Indian Ocean using the HOAPS data. Remote Sens Environ 80:363-372. doi:10.1016/S0034-4257(01)00302-9.

Ramesh Kumar MR, Shenoi SSC, Schulz J (2005) Impact of convection over the equatorial trough on summer monsoon activity over India. Int J Remote Sens 26:4747-4762. doi:10.1080/01431160500196414l.

Ramesh Kumar MR, Sreejith OP (2005) On some aspects of precipitation over the tropical Indian Ocean using satellite data. Int J Remote Sens 26:1717-1728. doi:10.1080/01431160412331331021.

Ramesh Kumar MR, Pednekar SM, Katsumata M, Antony MK, Kuroda Y, Unnikrishnan AS (2006) Seasonal variation of diurnal cycle of rainfall in the eastern equatorial Indian Ocean. Theor Appl Climatol 85:117-122. doi:10.1007/s00704-005-0179-3.

Ramesh Kumar MR, Krishnan R, Sankar S, Unnikrishnan AS, Pai DS (2009) Increasing trend of `Break-Monsoon` conditions over India – Role of ocean-atmosphere processes in the Indian Ocean. IEEE Geosci Remote Sens Lett 6:332-336. doi:10.1109/LGRS.2009.2013366.

Ramesh Kumar MR, Pinker RT, Mathew S, Venkatesan R, Chen W (2017) Evaluation of radiative fluxes over the north Indian Ocean. Theor Appl Climatol doi:10.1007/s00704-017-2141-6.

Sapiano MRP, Arkin PA (2009) An intercomparison and validation of high-resolution satellite precipitation estimates with 3-hourly gauge data. J Hydrometeorol 10:149-166. doi:10.1175/2008JHM1052.1.

Serra YL, A'Hearn P, Freitag P, McPhaden MJ (2001) ATLAS self-siphoning rain gauge error estimates. J Atmos Oceanic Technol 18:1989-2002.

Tapiador FJ, Navarro A, Levizzani V, Garcia-Ortega E, Huffman GJ, Kidd C, Kucera PA, Kummerow CD, Masunaga H, Petersen WA, Roca R, Sanchez J-L, Tao W-K, Turk FJ (2017) Global precipitation measurements for validating climate models. Atmos Res 197:1-20. doi:10.1016/j.atmosres.2017.06.021.

Trenberth KE, Smith L, Qian T, Dai A, Fasullo J (2007) Estimates of the global water budget and its annual cycle using observational and model data. J Hydrometeorol 8:758-769. doi:10.1175/JHM600.1.

Venkatesan R, Shamji VR, Latha G, Mathew S, Rao RR, Muthiah A, Atmanand MA (2013) In situ ocean subsurface time-series measurements from OMNI buoy network in the Bay of Bengal. Curr Sci 104:1166-1177.

Wang W, Lu H, Zhao T, Jiang L, Shi J (2017) Evaluation and comparison of daily rainfall from latest GPM and TRMM products over the Mekong river basin. IEEE J Select Topics Appl Earth Observ Remote Sens 10:2540-2549. doi:10.1109/JSTARS.2017.2672786.

Table 1: Error metrics obtained from the comparison of hourly precipitation from IMERG and OMNI buoys over the Arabian Sea and Bay of Bengal.

	Arabian Sea	**Bay of Bengal**
N	4032	29643
r	0.40	0.41
Bias (mm h^{-1})	0.13 (34%)	0.17 (38%)
RMSE (mm h^{-1})	2.68 (755%)	2.85 (646%)
Systematic Error	15%	13%
Random Error	85%	87%

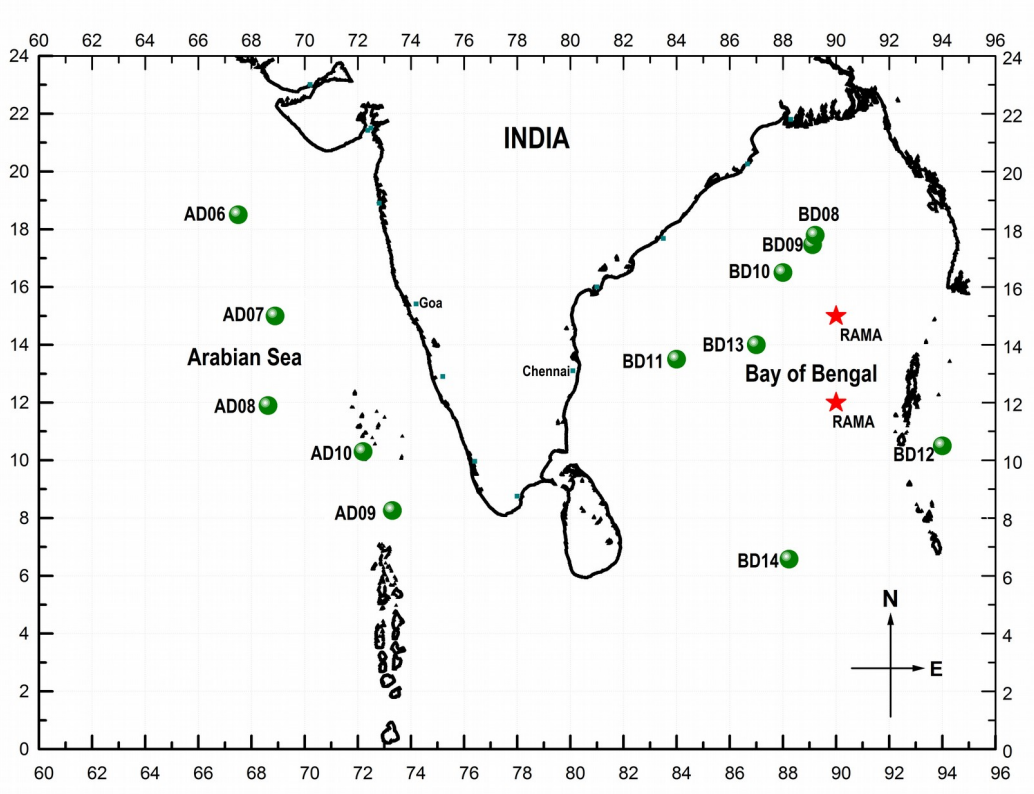

Figure 1: Locations of OMNI and RAMA buoys used in this study.

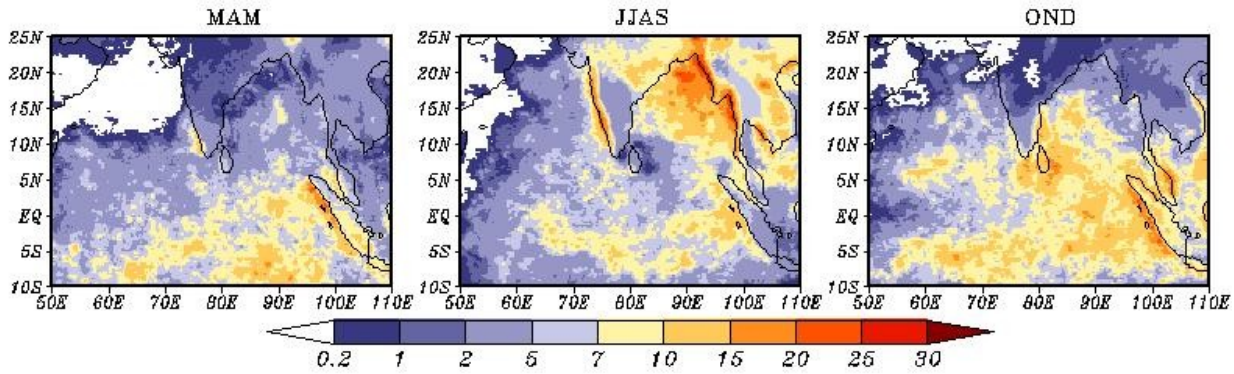

Figure 2: Seasonal precipitation (mm day^{-1}) over the north Indian Ocean derived from IMERG precipitation product for 2014 and 2015. MAM, JJAS, and OND represent the pre-monsoon (March – May), monsoon (June – September), and post-monsoon (October – December) seasons, respectively.

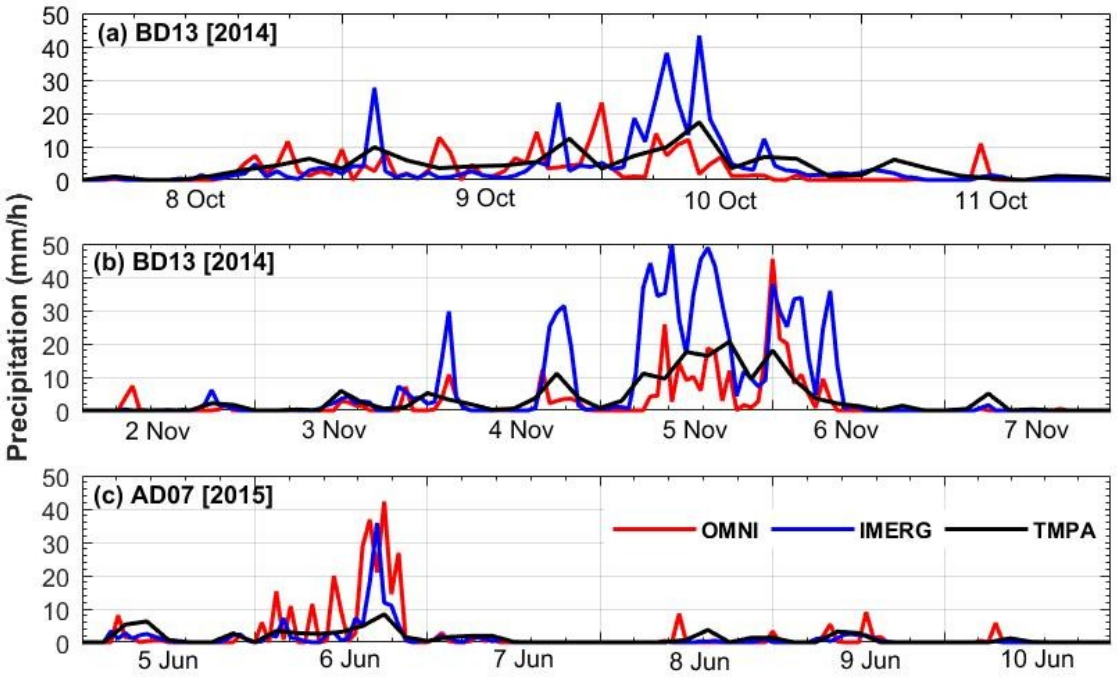

Figure 3: Time-series of hourly precipitation from OMNI buoys and from IMERG, and three-hourly precipitation from TMPA for (a) 8-11 October 2014 over the Bay of Bengal, (b) 2-7 November 2014 over the Bay of Bengal, and (c) 5-10 June 2015 over the Arabian Sea.

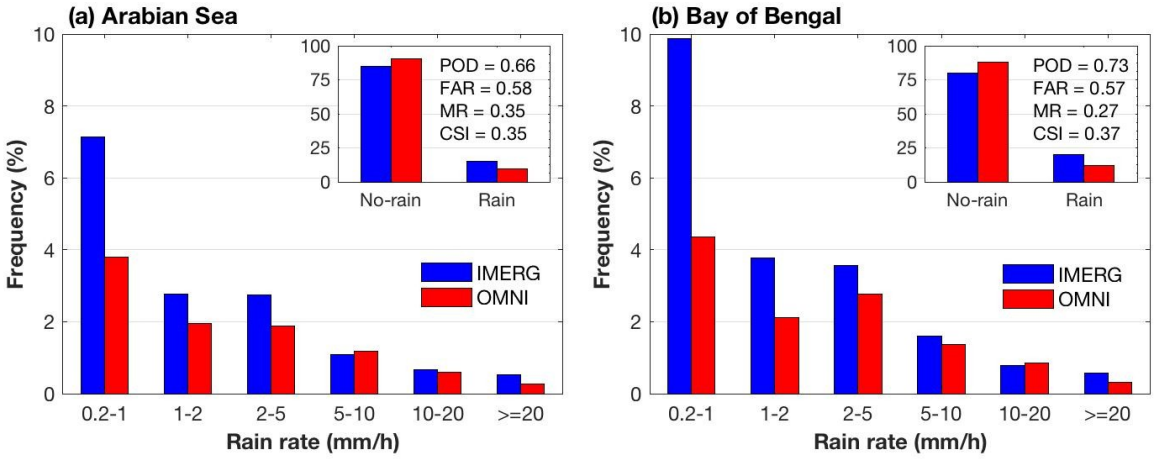

Figure 4: Percentage frequency of rain events from IMERG and OMNI buoy observations over the (a) Arabian Sea and (b) Bay of Bengal. The frequency of rain/no-rain events and their corresponding categorical metrics are also shown at the top-right corner of each plot.

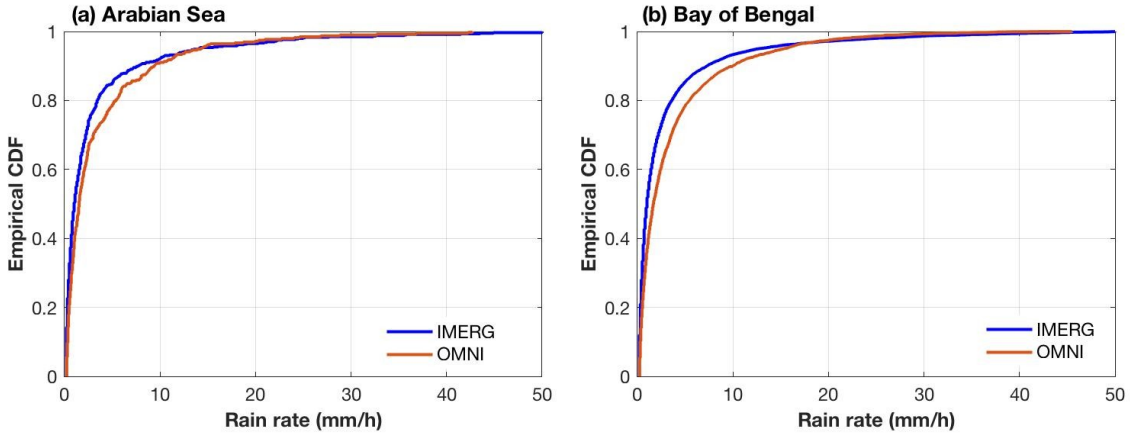

Figure 5: Empirical cumulative distribution functions of rainy events from IMERG and OMNI buoy observations over the (a) Arabian Sea and (b) Bay of Bengal.

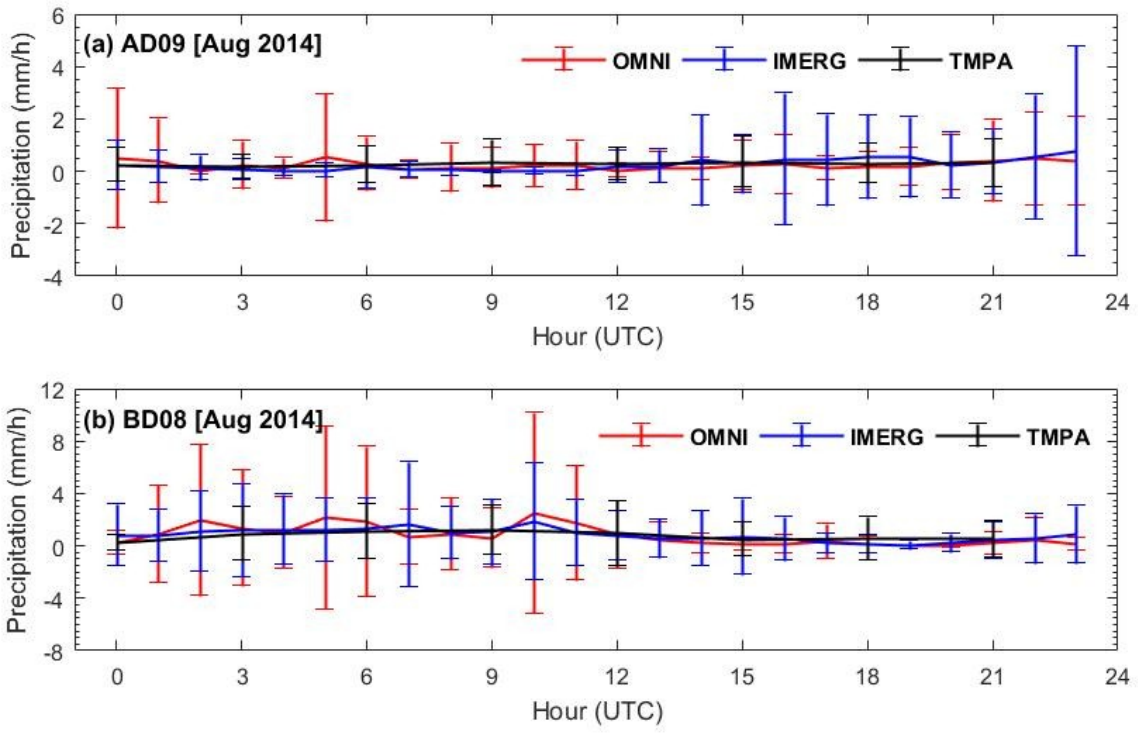

Figure 6: Diurnal variations of OMNI buoy, IMERG and TMPA precipitation for the month of August 2014 at selected location over the (a) Arabian Sea and (b) Bay of Bengal. The error bars represent their respective standard deviations.

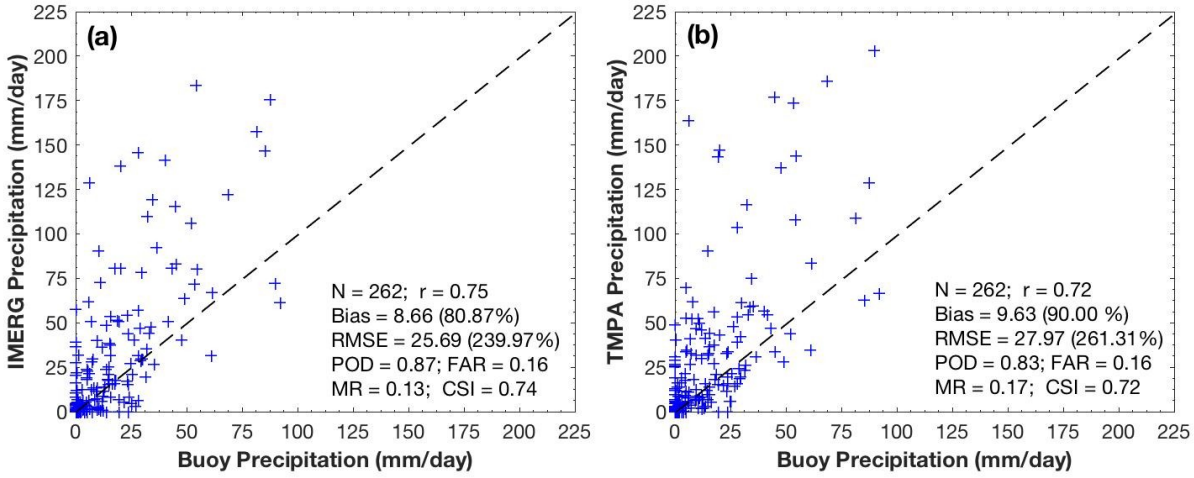

Figure 7: Scatter plots of daily precipitation between (a) IMERG and RAMA buoys, (b) TMPA and RAMA buoys for the southwest monsoon season of 2014-2015. The corresponding continuous and categorical metrics are also provided.